

Influence of Ice Compression on the Wave Current Velocities at the Nonlinear Interaction of Wave Harmonics

A. A. Bukatov

Marine Hydrophysical Institute of RAS, Sevastopol, Russian Federation

✉ bukatov.ant@mhi-ras.ru

Abstract

Purpose. The work is aimed at studying the ice compression influence on the components of fluid motion velocity under a floating ice cover in propagation of the wave formed by the nonlinear interaction of wave harmonics.

Methods and Results. Based on the obtained solution of the problem on nonlinear interaction of the progressive surface waves in a finite depth basin with floating and longitudinally compressed elastic ice, analyzed were the distributions of the components of fluid particles motion velocity along the generated wave length depending on the ice characteristics. The impact of thickness, elasticity modulus and compressive force of the ice cover, nonlinearity of the ice vertical acceleration and the amplitude of the second interacting harmonic upon the vertical and horizontal components of the fluid particles motion velocity was studied.

Conclusions. It is established that the compressive force conditions reduction of the phase and the maximum values of the fluid motion velocity components. Change in the sign of the second interacting harmonic amplitude is manifested in a significant profile transformation, and affects the generated perturbation phase at the regard for the nonlinearity of ice vertical acceleration. When the compression force value is fixed, a decrease in the ice cover rigidity results in a noticeable delay of the oscillation phase.

Keywords: nonlinear interaction of waves, flexural-gravity waves, longitudinal compressive force, waves of finite amplitude, motion of fluid particles, ice compression, ice cover

Acknowledgements: The investigation was carried out within the framework of the state task on theme FNNN-2021-0004.

For citation: Bukatov, A.A., 2023. Influence of Ice Compression on the Wave Current Velocities at the Nonlinear Interaction of Wave Harmonics. *Physical Oceanography*, 30(3), pp. 288-301. doi:10.29039/1573-160X-2023-3-288-301

DOI: 10.29039/1573-160X-2023-3-288-301

© A. A. Bukatov, 2023

© Physical Oceanography, 2023

Introduction

Waves propagate over considerable distances in the basins both with a free surface and with floating ice cover, which affects the dynamics of the sea surface and subsurface waters [1–3]. The ongoing climatic processes necessitate reliable calculations of wave characteristics and wave forecasts in ice conditions and require the development of theoretical studies, mathematical modeling, as well as field instrumental measurements and laboratory experiments [4–8]. When solving individual problems related to wave dynamics on the surface of a fluid, one should take into account the drift flow that occurs during the propagation of surface waves – the Stokes drift [9, 10]. Its velocity towards the direction of motion of finite amplitude waves was studied in [11–15] in the absence of ice cover. In [16, 17], the effect of floating broken ice on the rate of translational movement of a fluid in the direction towards the propagation of a progressive nonlinear wave was studied.



The study of the displacement velocity of fluid particles along the profile of a traveling periodic wave of finite amplitude in a basin with floating elastic ice was carried out in [18], and with continuous, longitudinally compressed elastic ice – in [19].

In this work, based on the obtained solution of the problem of nonlinear interaction of progressive surface waves in a basin of finite depth with floating longitudinally compressed elastic ice [20], we analyze the distributions of the velocity components of fluid particles along the length of the formed wave under the floating ice cover.

Problem statement

Let continuous, longitudinally compressed elastic ice with thickness $h = \text{const}$ float on the surface of a homogeneous ideal incompressible fluid of constant depth H . Liquid and ice cover in horizontal directions are not limited. We are to study ice effect on the orbital velocities of liquid particles, which are formed during the interaction of two wave harmonics of finite amplitude. We assume that the liquid movement is potential, and the oscillations of ice are continuous, then the task is to solve the Laplace equation

$$\varphi_{xx} + \varphi_{zz} = 0, \quad -\infty < x < \infty, \quad -H \leq z \leq \zeta \quad (1)$$

for the velocity potential with boundary conditions on the ice – liquid surface ($z = \zeta$)

$$D_1 k^4 \frac{\partial^4 \zeta}{\partial x^4} + Q_1 k^2 \frac{\partial^2 \zeta}{\partial x^2} + \kappa k \frac{\partial}{\partial z} \left[\frac{1}{2} \left(\frac{\partial \varphi}{\partial x} \right)^2 - \frac{\partial \varphi}{\partial t} \right] = p, \quad (2)$$

$$p = \frac{\partial \varphi}{\partial t} - \zeta - \frac{1}{2} \left[\left(\frac{\partial \varphi}{\partial x} \right)^2 + \left(\frac{\partial \varphi}{\partial z} \right)^2 \right]$$

and at the bottom ($z = -H$) of the basin

$$\frac{\partial \varphi}{\partial z} = 0. \quad (3)$$

At the initial moment of time ($t = 0$)

$$\zeta = f(x), \quad \frac{\partial \zeta}{\partial t} = 0. \quad (4)$$

The velocity potential and the elevation of ice – liquid surface at $z = \zeta$ are related by the kinematic condition

$$\frac{\partial \zeta}{\partial t} - \frac{\partial \zeta}{\partial x} \frac{\partial \varphi}{\partial x} + \frac{\partial \varphi}{\partial z} = 0. \quad (5)$$

Problem (1)–(5) is written in dimensionless quantities:

$$x = kx_1, \quad z = kz_1, \quad t = \sqrt{kg} t_1, \quad \zeta = k\zeta^*, \quad \varphi = \left(k^2 / \sqrt{kg} \right) \varphi^*.$$

Here

$$D_1 = \frac{D}{\rho g}, \quad D = \frac{Eh^3}{12(1-\nu^2)}, \quad Q_1 = \frac{Q}{\rho g}, \quad \kappa = h \frac{\rho_1}{\rho},$$

E, Q, h, ρ_1, ν are the modulus of normal elasticity, longitudinal compressive force, thickness, density, Poisson's ratio of ice, respectively; ρ is density of fluid; k is a wavenumber; g is gravitational acceleration; t is time; $\varphi(x, z, t)$ is a potential of fluid motion velocity; $\zeta(x, t)$ is an elevation of ice – fluid surface.

We note that in the dynamic condition (2), the expression with κ is the inertia of the vertical displacements of ice, the first term in parentheses of this expression characterizes the nonlinearity of ice vertical acceleration [20].

Expressions for the components of orbital velocity of fluid particles

The solution to the problem (1)–(5) was found by the multiscale method [21] in the form of equations for three approximations with regard to the nonlinearity of vertical displacement acceleration of longitudinally compressed elastic ice [20]. The first approximation of the basin surface elevation ζ_1 was set as

$$\zeta_1 = \cos \theta + a_1 \cos 2\theta, \quad \theta = x + \tau T_0 + \beta(T_1, T_2),$$

where a_1 is an amplitude of the second interacting harmonic, and $\beta(T_1, T_2)$ is determined from the second and third approximations. Here $T_1 = \varepsilon t$; $T_2 = \varepsilon^2 t$; $\varepsilon = ak$; a is an amplitude of initial harmonic. The final expression for the velocity potential in dimensionless variables, up to the third approximation, was found in the following form:

$$\begin{aligned} \varphi = & \varepsilon b_{11} \operatorname{ch}(z+H) \sin \theta + \sum_{n=1}^3 \varepsilon^n b_{n2} \operatorname{ch} 2(z+H) \sin 2\theta + \\ & + \sum_{n=2}^3 \varepsilon^n \sum_{j=3}^4 b_{nj} \operatorname{ch} j(z+H) \sin j\theta + \varepsilon^3 \sum_{n=5}^6 b_{3n} \operatorname{ch} n(z+H) \sin n\theta + \sum_{n=2}^3 \varepsilon^n b_{n0} t, \\ \theta = & x + \sigma t, \quad \sigma = \tau + \varepsilon \sigma_1 + \varepsilon^2 \sigma_2. \end{aligned}$$

Here

$$\tau^2 = (1 + D_1 k^4 - Q_1 k^2) (1 + \kappa k \operatorname{th} H)^{-1} \operatorname{th} H,$$

$$b_{11} = \frac{\tau}{\operatorname{sh} H}, \quad b_{12} = a_1 \frac{\tau}{\operatorname{sh} 2H},$$

$$b_{20} = \tau^2 \left(a_1^2 (1 + \operatorname{cth}^2 2H) + \frac{1}{4} (1 + \operatorname{cth}^2 H) + \kappa k \left(\frac{1}{2} \operatorname{cth} H + 4a_1^2 \operatorname{cth} 2H \right) \right),$$

$$b_{23} = \frac{l_3 \mu_3 + 3l_7 \tau}{3 \operatorname{sh} 3H (\mu_3 - 9\kappa k \tau^2 - 3\tau^2 \operatorname{cth} 3H)},$$

$$b_{24} = \frac{l_4 \mu_4 + 4l_8 \tau}{3 \operatorname{sh} 4H (\mu_4 - 16\kappa k \tau^2 - 4\tau^2 \operatorname{cth} 4H)},$$

$$\begin{aligned}
b_{30} &= a_1 \tau^2 \left(2\text{cth}2H + \frac{1}{2}\text{cth}H + \kappa k \left(\frac{9}{4} + 2\text{cth}2H\text{cth}H - \frac{1}{4}\text{cth}^2H \right) \right), \\
b_{3i} &= \frac{j_i \mu_i + i m_i \tau}{i \text{shi}H (\mu_i - i^2 \tau^2 \kappa k - i \tau^2 \text{cthi}H)}, \quad i = 3 \dots 6, \\
\mu_i &= 1 - i^2 Q l_i k^2 + i^4 D_1 k^4, \quad i = 1 \dots 6, \\
a_{23} &= \mu_3^{-1} (l_7 + 3\tau b_{23} (\text{ch}3H - \kappa k 3\text{sh}3H)), \\
a_{24} &= \mu_4^{-1} (l_8 + 4\tau b_{24} (\text{ch}4H - \kappa k 4\text{sh}4H)), \\
a_{3i} &= (i \tau b_{3i} (\text{chi}H + i \kappa k \text{shi}H) + m_i) \mu_i^{-1}, \quad i = 3 \dots 6, \\
a_1 &= \pm \left(\frac{\mu_2 r_1}{4r_2 (2\tau^2 \text{cth}2H + 4\tau^2 \kappa k + \mu_2) (1 + 2\kappa k \text{th}2H)} \right)^{1/2}, \\
r_1 &= \left(2\text{cth}H + \text{th}2H \left(\text{cth}H \left(\frac{1}{2}\text{cth}H + 3\kappa k \right) - \frac{5}{2} \right) \right) (\tau^2 (\text{cth}H + \kappa k) + \mu_1), \\
r_2 &= \tau^2 \left(\frac{1}{2} + \text{cth}2H \text{cth}H - \kappa k \left(\text{cth}2H - \frac{5}{2}\text{cth}H \right) \right) + \mu_1 \left(\frac{1}{2}\text{cth}H + \text{cth}2H \right), \\
l_3 &= -\frac{3}{2} a_1 \tau (2\text{cth}2H + \text{cth}H), \quad l_4 = -4a_1^2 \text{cth}2H, \\
l_7 &= a_1 \tau^2 \left(\frac{11}{2} - \text{cth}2H\text{cth}H + \kappa k \left(5\text{cth}2H - \frac{1}{2}\text{cth}H \right) \right), \\
l_8 &= a_1^2 \tau^2 (5 - \text{cth}^2 2H + 4\kappa k \text{cth}2H), \\
j_3 &= -\frac{5}{8} \tau - \frac{3}{8} a_1^2 \tau - 6b_{24} \text{ch}4H - \frac{3}{2} a_{24} \tau \text{cth}H + 3a_{23} \sigma_1, \\
j_4 &= -\frac{9}{2} a_1 \tau - 6b_{23} \text{ch}3H - 2a_{23} \tau \text{cth}H + 4a_{24} \sigma_1, \\
j_5 &= -\frac{69}{8} a_1^2 \tau - 10b_{24} \text{ch}4H - \frac{5}{2} a_{24} \tau \text{cth}H - 5a_1 \left(\frac{3}{2} b_{23} \text{ch}3H - a_{23} \tau \text{cth}2H \right), \\
j_6 &= -5a_1^3 \tau - 6a_1 (2b_{24} \text{ch}4H - a_{24} \tau \text{cth}2H),
\end{aligned}$$

$$\sigma_1 = \frac{\tau\mu_2 \left(2\text{cth}H + \text{th}2H \left(\text{cth}H \left(\frac{1}{2} \text{cth}H + 3\kappa k \right) - \frac{5}{2} \right) \right)}{4a_1 (2\tau^2 \text{cth}2H + 4\tau^2 \kappa k + \mu_2) (1 + 2\kappa k \text{th}2H)},$$

$$\sigma_2 = \frac{1}{4} \left(\frac{q_1}{\mu_1} + \frac{q_2}{2a_1\mu_2} \right),$$

$$m_3 = \tau \left(\frac{9}{2} a_1 \sigma_1 + 2b_{24} \text{ch}4H (2\text{th}4H - \text{cth}H) \right) + \\ + \frac{1}{2} \tau^2 \left(\frac{1}{4} \text{cth}H (1 - 23a_1^2) + 7a_1^2 \text{cth}2H - 3a_{24} \right) + 3b_{23} \sigma_1 \text{ch}3H + \\ + \kappa k \left(\tau \left(2b_{24} \text{sh}4H (1 \text{cth}4H - 4\text{cth}H) + 3a_1 \sigma_1 \left(2\text{cth}2H + \frac{1}{2} \text{cth}H \right) \right) \right) + \\ + \tau^2 \left(a_1^2 \left(\frac{21}{8} - 2\text{cth}^2 2H - \frac{7}{2} \text{cth}H \text{cth}2H \right) - \frac{1}{8} - \frac{3}{2} a_{24} \text{cth}H - \frac{1}{2} \text{cth}^2 H \right) + 9b_{23} \sigma_1 \text{sh}3H \Big),$$

$$m_4 = \tau \left(4\sigma_1 a_1^2 + \frac{3}{2} b_{23} \text{ch}3H (5\text{th}3H - \text{cth}H) \right) + 2\tau^2 \left(a_1 \text{cth}2H - \frac{1}{4} a_1 \text{cth}H + a_{23} \right) + \\ + 4b_{24} \sigma_1 \text{ch}4H + \kappa k \left(\tau \left(\frac{3}{2} b_{23} \text{sh}3H (1 \text{cth}3H - 3\text{cth}H) + 8a_1^2 \sigma_1 \text{cth}2H \right) \right) + \\ + \tau^2 \left(a_1 \left(\frac{37}{4} - 4\text{cth}2H \text{cth}H - \frac{3}{4} \text{cth}^2 H \right) + 2a_{23} \text{cth}H \right) + 16b_{24} \sigma_1 \text{sh}4H \Big),$$

$$m_5 = \tau \left(2b_{24} \text{ch}4H (6\text{th}4H - \text{cth}H) + 3b_{23} a_1 \text{ch}3H \left(\frac{7}{2} \text{th}3H - \text{cth}2H \right) \right) + \\ + \tau^2 \left(\frac{7}{2} a_1^2 \left(\text{cth}2H - \frac{1}{4} \text{cth}H \right) + 5a_{23} a_1 + \frac{5}{2} a_{24} \right) + \\ + \kappa k \left(\tau \left(2b_{24} \text{sh}4H (19\text{cth}4H - 4\text{cth}H) + 3b_{23} a_1 \text{sh}3H \left(\frac{11}{2} \text{cth}3H - 3\text{cth}2H \right) \right) \right) + \\ + \tau^2 \left(-a_1^2 \left(\frac{3}{8} + 6\text{cth}^2 2H + \frac{11}{2} \text{cth}2H \text{cth}H \right) + 10a_{23} a_1 \text{cth}2H + \frac{5}{2} a_{24} \text{cth}H \right) \Big),$$

$$m_6 = 4\tau b_{24} a_1 \text{ch}4H (4\text{th}4H - \text{cth}2H) + \tau^2 a_1 (a_1^2 \text{cth}2H + 6a_{24}) + \\ + 2\kappa k a_1 \left(4\tau b_{24} \text{sh}4H (5\text{cth}4H - 2\text{cth}2H) + \tau^2 (6a_{24} \text{cth}2H - a_1^2 (1 + 4\text{cth}^2 2H)) \right) \Big),$$

$$\begin{aligned}
q_1 = & \mu_1 \left(\frac{3}{2} b_{23} a_1 \operatorname{ch} 3H - \tau \left(\frac{3}{8} - \frac{15}{4} a_1^2 + a_{23} a_1 \operatorname{cth} 2H \right) \right) + \tau^2 a_1 \left(-\frac{1}{2} \sigma_1 + \right. \\
& + 3b_{23} \operatorname{ch} 3H \left(\frac{1}{2} \operatorname{th} 3H + \operatorname{cth} 2H \right) \left. \right) + \tau^3 \left(9a_1^2 \operatorname{cth} 2H + a_1 a_{23} + \frac{1}{4} \operatorname{cth} H \left(\frac{5}{2} - a_1^2 \right) \right) + \\
& + \kappa k \left(\tau^2 a_1 \left(3b_{23} \operatorname{sh} 3H \left(\frac{1}{2} \operatorname{cth} 3H + 3 \operatorname{cth} 2H \right) - 2\sigma_1 \operatorname{cth} 2H + \frac{1}{2} \sigma_1 \operatorname{cth} H \right) + \right. \\
& \left. + \tau^3 \left(2a_{23} a_1 \operatorname{cth} 2H + \frac{1}{2} \operatorname{cth}^2 H + \frac{3}{8} + a_1^2 \left(8 \operatorname{cth}^2 2H + \operatorname{cth} H \operatorname{cth} 2H + \frac{39}{4} \right) \right) \right),
\end{aligned}$$

$$\begin{aligned}
q_2 = & \mu_2 \left(3b_{23} \operatorname{ch} 3H + 4b_{24} a_1 \operatorname{ch} 4H + \tau \left(a_{23} \operatorname{cth} H + 2a_{24} a_1 \operatorname{cth} 2H - 3a_1^3 \right) \right) + \\
& + 2\tau^2 \left(\frac{3}{2} b_{23} \operatorname{ch} 3H \left(\operatorname{cth} H - \operatorname{th} 3H \right) + 4b_{24} a_1 \operatorname{cth} 2H \operatorname{ch} 4H - \sigma_1 \right) + \\
& + 2\tau^3 \left(a_{23} + a_1 \left(3a_1 \operatorname{cth} H + 2a_{24} + \operatorname{cth} 2H \left(5a_1^2 - 2 \right) \right) \right) + \\
& + \kappa k \left(2\tau^2 \left(\frac{3}{2} b_{23} \operatorname{sh} 3H \left(3 \operatorname{cth} H - 5 \operatorname{cth} 3H \right) + 8b_{24} a_1 \operatorname{sh} 4H \left(2 \operatorname{cth} 2H - \operatorname{cth} 4H \right) - \sigma_1 \operatorname{cth} H \right) + \right. \\
& \left. + 2\tau^3 \left(2a_1^3 \left(3 + 4 \operatorname{cth} 2H \right) + a_1 \left(4 \operatorname{cth} 2H \left(a_{24} + \operatorname{cth} H \right) + \frac{1}{2} \operatorname{cth}^2 H - \frac{3}{2} \right) + a_{23} \operatorname{cth} H \right) \right).
\end{aligned}$$

Thus $b_{22} = b_{32} = a_2 = a_3 = l_1 = l_2 = l_5 = l_6 = j_1 = j_2 = m_1 = m_2 = 0$.

In dimensional variables, the expression for the velocity potential has the form

$$\begin{aligned}
\varphi = & a\sqrt{g/k} \sum_{n=1}^2 b_{1n} \operatorname{ch} nk(z+H) \sin n\theta + a^2 \sqrt{kg} \left(\sum_{n=3}^4 b_{2n} \operatorname{ch} nk(z+H) \sin n\theta + b_{20} t \right) + \\
& + a^3 k \sqrt{kg} \left(\sum_{n=3}^6 b_{3n} \operatorname{ch} nk(z+H) \sin n\theta + b_{30} t \right),
\end{aligned} \tag{6}$$

$$\theta = kx + \sqrt{kg} \left(\tau + ak\sigma_1 + a^2 k^2 \sigma_2 \right) t,$$

and in the expressions for b_{20} , b_{30} , b_{11} , b_{12} , b_{23} , b_{24} , b_{33} , b_{34} , b_{35} , b_{36} , σ_1 , σ_2 the argument of hyperbolic functions is replaced by kH . Here and below, for expressions in dimensional variables, the symbols “ x ”, “ z ”, “ t ” have index 1 omitted, and “ φ ” – the sign “*”. Consequently, the horizontal (u) and vertical (w) components of a homogeneous fluid velocity, taking into account formula (6), are determined by the expressions

$$\begin{aligned}
u = & a\sqrt{kg} \sum_{n=1}^2 n b_{1n} \operatorname{ch} nk(z+H) \cos n\theta + a^2 k \sqrt{kg} \sum_{n=3}^4 n b_{2n} \operatorname{ch} nk(z+H) \cos n\theta + \\
& + a^3 k^2 \sqrt{kg} \sum_{n=3}^6 n b_{3n} \operatorname{ch} nk(z+H) \cos n\theta,
\end{aligned}$$

$$w = a\sqrt{kg} \sum_{n=1}^2 nb_{1n} \operatorname{sh} nk(z+H) \sin n\theta + a^2 k \sqrt{kg} \sum_{n=3}^4 nb_{2n} \operatorname{sh} nk(z+H) \sin n\theta + a^3 k^2 \sqrt{kg} \sum_{n=3}^6 nb_{3n} \operatorname{sh} nk(z+H) \sin n\theta.$$

Note that the resulting solution is valid outside small neighborhoods of the resonant values of the wavenumbers k_i ($i = 1 \dots 4$) [20].

Analysis of the dependence of fluid velocity components on ice cover characteristics

To assess the effect of ice cover characteristics on the velocity of wave currents under the ice, numerical calculations were performed at $\rho_1/\rho = 0.87$; $\nu = 0.34$; $0 \leq h \leq 2$ m; E equal to 0; $5 \cdot 10^8$; 10^9 ; $3 \cdot 10^9$ N/m², and the condition $Q_1 < 2\sqrt{D}$ necessary for the stability of the floating ice cover¹ [22].

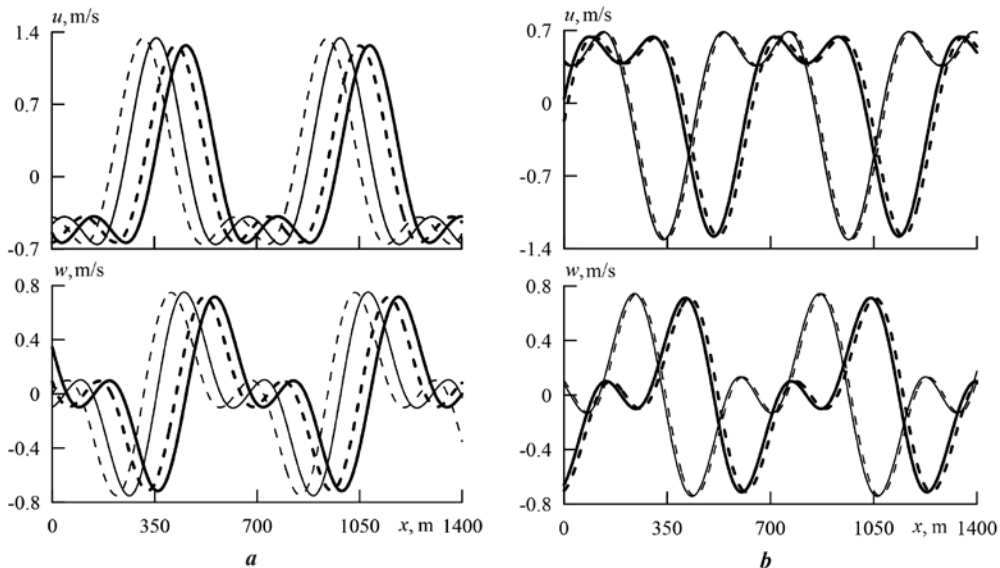


Fig. 1. Distribution of the fluid motion velocity components under ice compression $Q_1 = \sqrt{D}$ (thick lines) and in its absence $Q_1 = 0$ (thin lines) for the case when $a_1 > 0$ (a) and $a_1 < 0$ (b) at $\lambda/H = 10.47$. Dashed lines are obtained with allowance for ice vertical acceleration; solid ones – without it

Fig. 1 gives the distribution of horizontal and vertical velocity components under the conditions of ice compression, $Q_1 = \sqrt{D}$, and in its absence, $Q_1 = 0$, for the case $a_1 > 0$ (Fig. 1, a) and $a_1 < 0$ (Fig. 1, b). Here $E = 3 \cdot 10^9$ N/m², $H = 60$ m, $a = 2$ m, $h = 2$ m, wavelength $\lambda = 628$ m. In Fig. 1, a, it can be seen that during the propagation of a wave formed during the nonlinear interaction of two harmonics, the compressive force effect is manifested in a noticeable decrease in

¹ Kheisin, D.E., 1967. *Dynamics of Ice Cover*. L.: Gidrometeoizdat, 215 p. (in Russian).

the phase and maximum values of the fluid velocity components. Consideration of the nonlinearity of ice vertical acceleration manifests itself in the acceleration of the generated perturbation displacement compared to the profile constructed without taking it into account. This trend remains even in the presence of a compression force. The sign change of the amplitude of the second interacting harmonic from minus to plus leads to a qualitative and quantitative profile transformation (Fig. 1, *b*). The effect of the compressive force remains, however, the nonlinearity of the acceleration of floating ice vertical displacements manifests itself in a decrease in the phase of the wave profile.

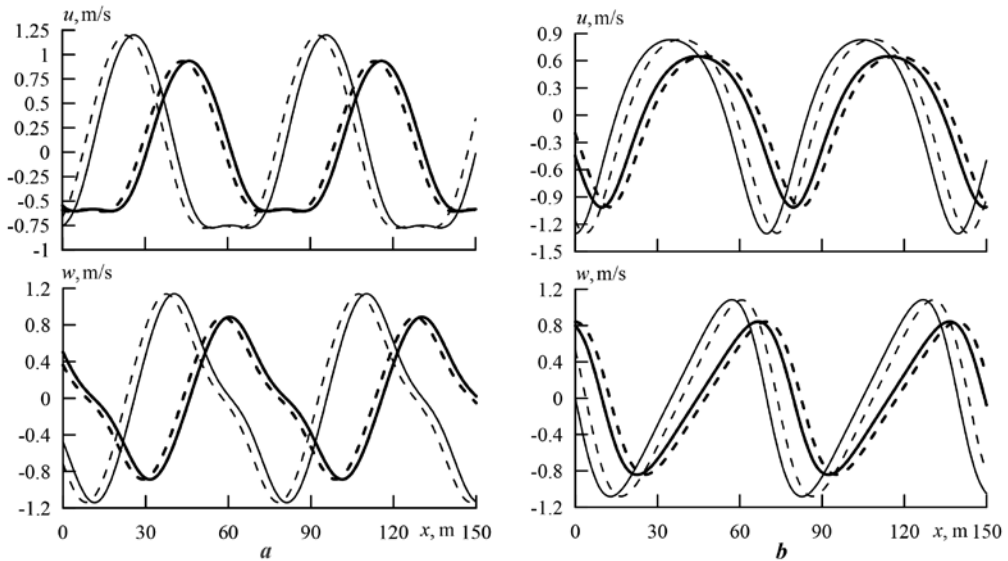


Fig. 2. Distribution of fluid motion velocity components under ice compression $Q_1 = \sqrt{D}$ (thick lines) and in its absence $Q_1 = 0$ (thin lines) for the case when $a_1 > 0$ (*a*) and $a_1 < 0$ (*b*) at $\lambda/H = 0.69$. Dashed lines are obtained with allowance for ice vertical acceleration; solid ones – without it

For the range of short waves (Fig. 2), the ice cover impact in the presence of a compressive force is more noticeable, compared to long waves, in the phase shift and amplitude values of the fluid velocity components. The profiles of the generated perturbations are nonlinear. Here $E = 3 \cdot 10^9$ N/m², $H = 100$ m, $a = 1$ m, $h = 0.5$ m, $Q_1 = \sqrt{D}$, $\lambda \approx 69$ m. Note that the values of the vertices on the horizontal velocity component profile $u(x)$ for the studied wave disturbances, as well as in the case of the interaction of wave harmonics in a basin with an elastic ice cover [23], in the linear case and during the propagation of periodic flexural-gravity waves of finite amplitude [18, 19] correspond to the values $w(x) = 0$. In this case, the values of the vertices on $w(x)$ profile correspond to the values $u(x) \neq 0$.

The compression force effect on the orbital motion velocity components of liquid particles with a change in the modulus of elasticity is shown in Fig. 3 at $a_1 > 0$ (Fig. 3, *a*) and $a_1 < 0$ (Fig. 3, *b*). Here $H = 100$ m, $a = 1$ m, $h = 0.6$ m, $Q_1 = \sqrt{D}$, $E = 3 \cdot 10^9$ N/m² (solid line), $E = 10^9$ N/m² (dashed line), $E = 5 \cdot 10^8$ N/m² (dashed-

dotted line). The profiles of velocity components are constructed with allowance for the inertia of the vertical ice displacements. It can be seen from the figure that with a decrease in the ice cover rigidity, a noticeable delay in the oscillation phase occurs. At the same time, its amplitude also decreases. When the sign of the second interacting harmonic changes, the profiles of the velocity components are deformed qualitatively and quantitatively. The change in the modulus of ice elasticity affects the distribution of velocity components in the same way.

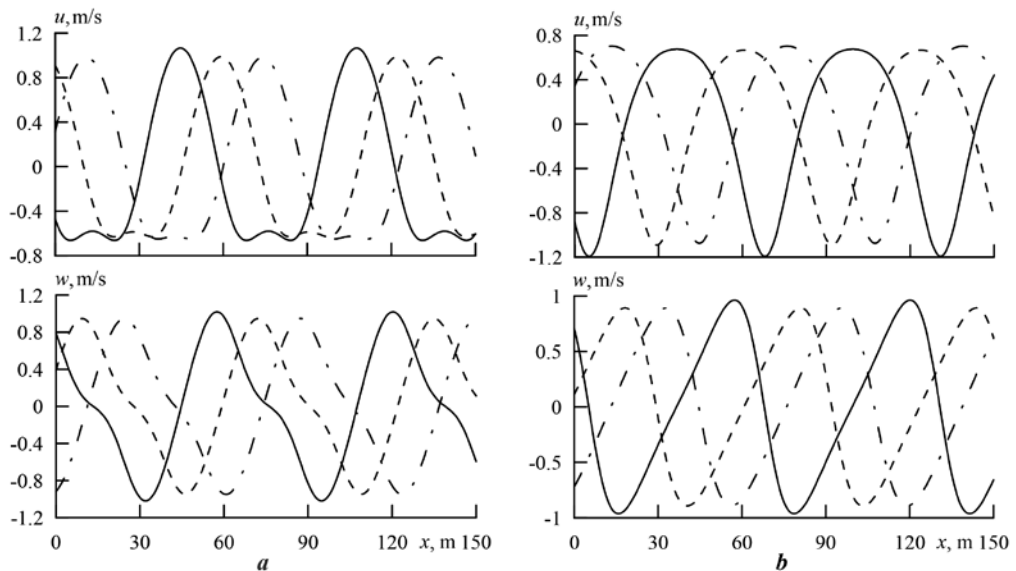


Fig. 3. Distribution of fluid motion velocity components under ice compression $Q_1 = \sqrt{D}$ for the case when $a_1 > 0$ (a) and $a_1 < 0$ (b). Solid line corresponds to $E = 3 \cdot 10^9$ N/m², dashed line – to $E = 10^9$ N/m², and dash-dotted one – to $E = 5 \cdot 10^8$ N/m²

The distribution of the ratio of maximum values along the wavelength of the vertical (W) and horizontal (U) velocity component over the wave number in the case of taking into account the nonlinearity of ice vertical acceleration is demonstrated in Fig. 4. The range of considered wave numbers is located outside the resonant values [20]. Here $H = 60$ m, $a = 1$ m, $h = 1$ m, $E = 3 \cdot 10^9$ N/m². It can be seen that in the considered range of k , the wave number distribution W/U is less than unity; therefore, as in the case of the propagation of a nonlinear periodic wave [18, 19], the vertical component does not exceed the horizontal velocity component. In contrast to the linear case, the distribution of the W/U ratio within the range of small k is not monotonic; here, the manifestation of the compressive force and the influence of the sign of the second interacting harmonic amplitude are noticeable. Note that, in this range, a decrease in the Young's modulus affects the decrease in the ratio both at $Q_1 \neq 0$ and at $Q_1 = 0$. As k increases, the sign of the amplitude a_1 has the greatest effect on W/U .

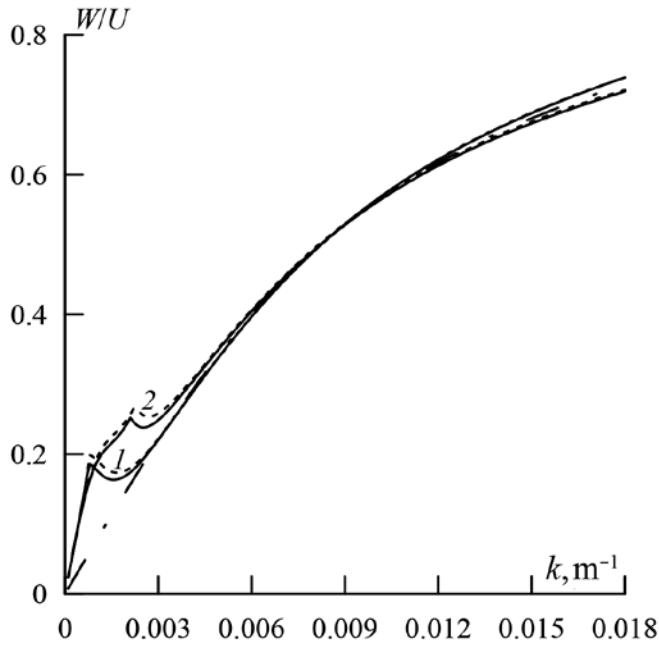


Fig. 4. Distribution of the W/U ratio value over the wave number. Solid lines – $Q_1 = \sqrt{D}$; dashed lines – $Q_1 = 0$ and dash-dotted one is a linear case. Lines 1 correspond to the case when $a_1 > 0$, and lines 2 – when $a_1 < 0$

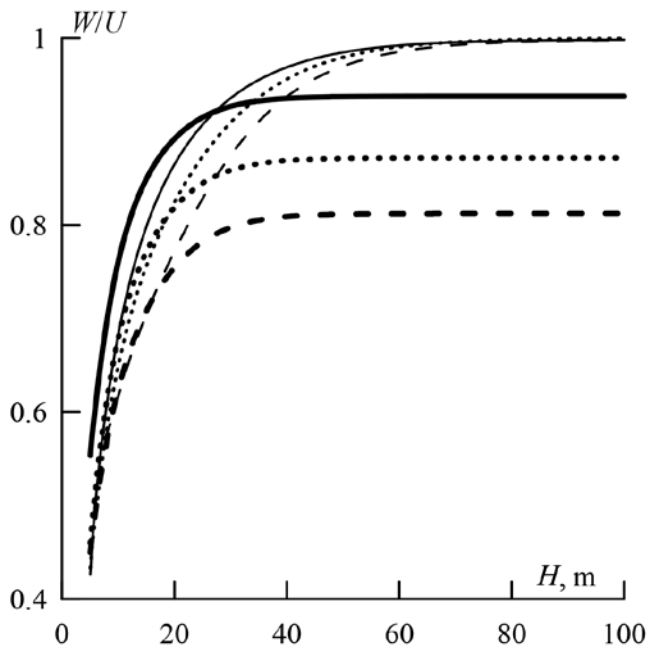


Fig. 5. Distribution of the W/U ratio value over the fluid depth at $\lambda = 78.5$ m. Thick lines – $h = 1$ m, $E = 3 \cdot 10^9$ N/m², $Q_1 = \sqrt{D}$; thin ones – $h = E = Q_1 = 0$. Solid lines correspond to the case when $a_1 > 0$, dashed lines – when $a_1 < 0$, and dotted ones correspond to the linear case

The dependence of the ratio of the maximum wavelength values that make up the velocity on the basin depth for a given wavelength λ is given in Fig. 5, with allowance for the nonlinearity of ice vertical acceleration. It can be seen that in the presence of ice cover, with increasing basin depth, the ratio of the vertical and horizontal velocity components ($W/U_{h \neq 0}$) increases and at $H > 40$ m the ratio remains almost constant. The value of $W/U_{h \neq 0}$ depends on the sign of the second interacting harmonic and can be either greater than the value of this ratio in the linear case, or less than it. In the absence of ice cover, the value $W/U_{h \neq 0} \sim \text{const}$ at $H > 80$ m. It can be seen from the presented distributions that, starting from $H > 40$ m, $W/U_{h \neq 0} < W/U_{h=0} < 1$, i.e. the vertical component does not exceed horizontal one, and the presence of a continuous longitudinally compressed elastic ice cover reduces the value of the ratio compared with the case of no ice. Note that with an increase in the initial harmonic amplitude, for $a_1 > 0$, the W/U ratio increases, and for $a_1 < 0$, it decreases. With a decrease in the elastic modulus at $Q_1 = 0$, the ratio slightly increases both at $a_1 > 0$ and at $a_1 < 0$. Moreover, at $a_1 < 0$, it is more noticeable. The compressive force effect on the W/U ratio depends on the value of normal elasticity modulus, for example, at $H > 40$ m, $Q_1 = \text{const}$ and decreasing E , the W/U ratio increases.

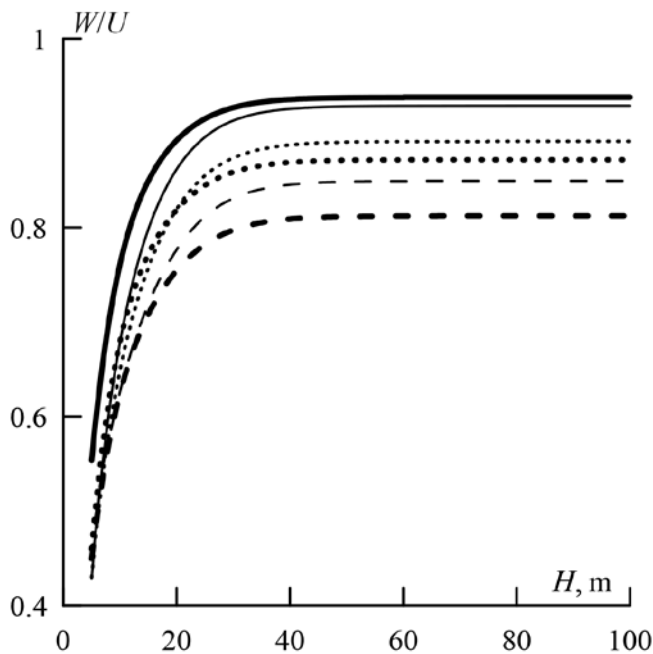


Fig. 6. Distribution of the W/U ratio value over the fluid depth at $\lambda = 78.5$ m. Thick lines – $h = 1$ m, $E = 3 \cdot 10^9$ N/m², $Q_1 = \sqrt{D}$; thin ones – $h = 1$ m, $E = Q_1 = 0$. Solid lines correspond to the case when $a_1 > 0$, dashed lines – when $a_1 < 0$, and dotted ones correspond to the linear case

Distribution of W/U dependence over depth H at $\lambda = 78.5$ m for the case of absolutely flexible ice ($h \neq 0$, $E = Q_1 = 0$) and the case of elastic longitudinally compressed ice ($h \neq 0$, $E \neq 0$, $Q_1 \neq 0$) is demonstrated in Fig. 6 when taking into account nonlinearity of the acceleration of its vertical displacements. Thick lines, as in Fig. 5 correspond to the case of an elastic longitudinally compressed ice cover

($h = 1$ m, $E = 3 \cdot 10^9$ N/m², $Q_1 = \sqrt{D}$, $a = 1$ m). Thin lines are the case of absolutely flexible ice (broken ice), here $h = 1$ m, $E = Q_1 = 0$, $a = 1$ m. Solid lines – $a_1 > 0$, dashed lines – $a_1 < 0$, dotted lines – linear case. It can be seen that, starting from $H > 30$ m, the W/U distributions for the case of broken ice ($W/U_{E=0}$) \sim const and are inside the distribution for elastic, longitudinally compressed ice ($W/U_{Q_1 \neq 0}$) \sim const, this is also preserved in the case of elastic ice ($Q_1 = 0$). For the case when $a_1 > 0$, $W/U_{E=0} < W/U_{Q_1 \neq 0}$, and for the linear case and the case when $a_1 < 0$, $W/U_{Q_1 \neq 0} < W/U_{E=0}$. Note that the effect of taking into account the nonlinearity of the ice vertical acceleration on the W/U ratio with increasing basin depth is most noticeable in the case of absolutely flexible ice. At $a_1 > 0$, the value of the W/U ratio decreases, and at $a_1 < 0$ it increases, and the effect of ice acceleration nonlinearity is more noticeable at $a_1 < 0$.

Conclusion

Based on the obtained solution of the problem of progressive surface wave nonlinear interaction in a basin of finite depth with floating longitudinally compressed elastic ice, an analysis of the distributions of velocity components of fluid particle motion along the length of the formed wave under the floating ice cover was carried out. The effect of the thickness, elastic modulus and compressive force of the ice cover, with allowance for nonlinearity of ice vertical acceleration, the amplitude of the second interacting harmonic on the vertical and horizontal components of the liquid particle velocity is studied.

It is found that the compressive force causes a decrease in the phase and the maximum values of the fluid velocity components. The change in the sign of the amplitude of the second interacting harmonic manifests itself in a significant transformation of the profile and affects the phase of generated perturbation when nonlinearity of the ice vertical acceleration is taken into account. At a fixed value of the compression force, a decrease in the ice cover rigidity leads to a noticeable delay in the oscillation phase.

The distribution of maximum values ratio of the vertical and horizontal velocity components along the wavelength over the wave number within the range of small wave numbers is not monotonous – manifestation of compressive force and the influence of the sign of the second interacting harmonic amplitude are noticeable in comparison with the linear case. For a given wavelength, there is a difference in the ratio values for the cases of an open surface, broken ice, and continuous, longitudinally compressed elastic ice. There is a depth value, starting from which, for all considered cases, the ratios of the vertical and horizontal velocity components remain practically constant and less than unity.

REFERENCES

1. Squire, V.A., 2007. Of Ocean Waves and Sea-Ice Revisited. *Cold Regions Science and Technology*, 49(2), pp. 110-133. doi:10.1016/j.coldregions.2007.04.007
2. Takagi, K., 1997. Interaction between Solitary Wave and Floating Elastic Plate. *Journal of Waterway, Port, Coastal, and Ocean Engineering*, 123(2), pp. 57-62. doi:10.1061/(ASCE)0733-950X(1997)123:2(57)

3. Bukatov, A.E., 2017. *Waves in the Sea with a Floating Ice Cover*. Sevastopol: MHI, 360 p. (in Russian).
4. Shen, H.H., 2022. Wave-Ice Interaction Models and Experimental Observations. In: J. Tuhkuri and A. Polojärvi, eds., 2022. *IUTAM Symposium on Physics and Mechanics of Sea Ice*. Cham: Springer, pp. 183-200. doi:10.1007/978-3-030-80439-8_9
5. Smirnov, V.N., Kovalev, S.M., Nubom, A.A. and Znamenskiy, M.S., 2020. Mechanics of Oscillations and Waves in the Ice of the Arctic Ocean during Compression and Ridging. *Arctic and Antarctic Research*, 66(3), pp. 321-336. doi:10.30758/0555-2648-2020-66-3-321-336 (in Russian).
6. Sui, J., Wang, J., He, Y. and Krol, F., 2010. Velocity Profiles and Incipient Motion of Frazil Particles under Ice Cover. *International Journal of Sediment Research*, 25(1), pp. 39-51. doi:10.1016/S1001-6279(10)60026-1
7. Ogasawara, T. and Sakai, S., 2006. Numerical Analysis of the Characteristics of Waves Propagating in Arbitrary Ice-Covered Sea. *Annals of Glaciology*, 44, pp. 95-100. doi:10.3189/172756406781811402
8. Korobkin, A.A., Papin, A.A. and Khabakhpasheva, T.I., 2013. [*Mathematical Models of the Snow-Ice Cover*]. Barnaul: Altai State University, 116 p. (in Russian).
9. Stokes, G., 2009. On the Theory of Oscillatory Waves. In: G. Stokes, 2009. *Mathematical and Physical Papers*. Cambridge: Cambridge University Press, pp. 197-229. doi:10.1017/CBO9780511702242
10. Curcic, M., Chen, S.S. and Özgökmen, T.M., 2016. Hurricane-Induced Ocean Waves and Stokes Drift and Their Impacts on Surface Transport and Dispersion in the Gulf of Mexico. *Geophysical Research Letters*, 43(6), pp. 2773-2781. doi:10.1002/2015GL067619
11. Nesterov, S.V., 1968. Generation of the Surface Waves of Finite Amplitude by the Running System of Pressure. *Izvestiya Akademii Nauk SSSR. Fizika Atmosfery i Okeana*, 4(10), pp. 1123-1125 (in Russian).
12. Newman, J.N., 1977. *Marine Hydrodynamics*. Cambridge: MIT Press, 402 p.
13. Longuet-Higgins, M., 1987. Lagrangian Moments and Mass Transport in Stokes Waves. *Journal of Fluid Mechanics*, 179, pp. 547-555. doi:10.1017/S0022112087001654
14. Aleshkov, Yu.Z., 1996. [*Currents and Waves in the Ocean*]. Saint Petersburg: St. Petersburg University, 224 p. (in Russian).
15. Bukatov, Ant.A., and Bukatova, O.M., 2011. Velocities of Fluid Motion in a Traveling Periodic Wave of Finite Amplitude. In: MHI, 2011. *Monitoring Systems of Environment*. Sevastopol: MHI. Iss. 11, pp. 269-271 (in Russian).
16. Bukatov, A.E. and Zharkov, V.V., 2001. Influence of Broken Ice upon Velocity of Wave Currents when Progressive Waves Pass above the Bottom Stagger. *Morskoy Gidrofizicheskiy Zhurnal*, (5), pp. 3-14 (in Russian).
17. Bukatov, A.E. and Bukatov, A.A., 1999. Propagation of Surface Waves of Finite Amplitude in a Basin with Floating Broken Ice. *International Journal of Offshore and Polar Engineering*, 9(3), pp. 161-166.
18. Bukatov, Ant.A. and Bukatov, And.A., 2011. Velocities of Motion of Liquid Particles under the Floating Ice Cover in the Case of Propagation of Periodic Waves of Finite Amplitude. *Physical Oceanography*, 21(1), pp. 13-22. doi:10.1007/s11110-011-9100-z
19. Bukatov, Ant.A. and Bukatova, O.M., 2011. Influence of Ice Compression on Components of the Velocity of Motion of Liquid under the Ice Cover in a Traveling Periodic Flexural Gravity Wave of Finite Amplitude. *Physical Oceanography*, 21(4), pp. 245-253. doi:10.1007/s11110-011-9119-1
20. Bukatov, A.A., 2019. Nonlinear Vibrations of a Floating Longitudinally Compressed Elastic Plate in the Interaction of Wave Harmonics of Finite Amplitude. *Fluid Dynamics*, 54(2), pp. 194-204. doi:10.1134/S0015462819020046
21. Nayfeh, A.H., 1973. *Perturbation Methods*. Chichester: John Wiley & Sons, 425 p.

22. Bukatov, A.E., 1981. Effect of Longitudinal Compression on Transient Vibrations of an Elastic Plate Floating on the Surface of a Liquid. *Soviet Applied Mechanics*, 17(1), pp. 75-79. doi:10.1007/BF00885650
23. Bukatov, A.A., 2022. Velocity of the Wave Currents under the Floating Elastic Ice Formed by Nonlinear Interaction of the Wave Harmonics. *Physical Oceanography*, 29(1), pp. 3-14. doi:10.22449/1573-160X-2022-1-3-14

About the author:

Anton A. Bukatov, Leading Research Associate, Marine Hydrophysical Institute of RAS (2 Kapitanskaya Str., Sevastopol, 299011, Russian Federation), Ph.D. (Phys.-Math.), **ORCID ID: 0000-0002-1165-8428**, **ResearcherID: P-6733-2017**, bukatov.ant@mhi-ras.ru

The author has read and approved the final manuscript.

The author declares that he has no conflict of interest.